International Journal of Environment Volume : 06 | Issue : 02 | April-June | 2017
ISSN: 2077-4508 Pages: 42-60

Thermodynamic and Kinetic Studies on the Cadmium Removal from Synthetic and Real Contaminated Water by Means of Amberjet 1500H Resin

A.A. Swelam, M.B. Awad, A.M.A. Salem and M.G. Gab-Allah

Chemistry Department, Faculty of Science, Al-Azhar University, Cairo*, Egypt.*

Received: 12 March 2017 / Accepted: 30 April 2017 / Publication Date: 04 May 2017

ABSTRACT

The most ideal conditions for the adsorption of Cd (II) ions onto Amberjet 1500H strong cation exchange resin from aqueous solution were investigated. The effects of four adsorption variables (temperature, resin dose, solution acidity and initial cadmium concentration) were studied. The equilibrium behavior has been modelized by means of Langmuir, Freundlich, Temkin and D-R isotherms. It was found that Langmuir isotherm and pseudo-second-order kinetics provides the most accurate prediction of the experimental data ($R^2 > 0.99$). Results reveal that the adsorption process is spontaneous (negative value of $\Delta G°$). Cadmium IE process was found to undergo pseudo-second order kinetics, as supported by the high square fit ($R^2 > 0.999$) and low sum of squared error values. The salt effect (NaCl, $NaNO_3$, Na-acetate and Na-citrate) on the removal of Cd(II) was also investigated at different salt concentrations. There was decrease in cadmium removal efficiency with increase of salt concentration. Furthermore, thermodynamic constant values (ΔG, ΔH and ΔS) were also studied herein in addition to Ea and S^*. Results of this work demonstrated the potential use of the resin for Cd(II) removal from industrial wastewater.

Key words: *Cadmium;* Adsorption; Removal; Kinetics; Thermodynamic

Introduction

Removal of heavy metals is a great challenge in waste water treatment processes. Industrial activities including mining, painting and coating, battery manufacturing generate sizable quantities of effluents conveying high levels of heavy metals (Apak*et al*., 1998). Such metals pose considerable threat to human health and ecological systems due to their persistence in the environment and the lack of low-cost technologies to remove those (McManamon *et al*., 2012). In particular, according to the World Health Organization (WHO 2007), cadmium is considered as a potential cause of kidney and bone damages and as a serious human carcinogen WHO, 2008 limited the maximum concentration of cadmium in drinking water to 0003 mg/l

The effluents containing cadmium are produced in industries including metal plating, batteries, plastic, pigments, nonferrous mining and smelting, *etc.*, (Elkady *et al*., 2011) which migrating into water sources and farmlands pose a serious threat to plants, animals and even human beings because of the bioaccumulation, irreversibility and toxicity of cadmium ion. Thus, scholars have paid much attention for the removal and recovery of cadmium, and various methods. Among the different methods described above, adsorption process is attractive due to its merits of efficiency, economy and simple operation, and lots of studies on this process have been carried out (Ensieh *et al*., 2017; Zahra *et al*., 2017; Rajab *et al*., 2017; Mohammad *et al*., 2017; Edidiong *et al*., 2017; Bruno *et al*., 2017; Joyce *et al*., 2017; Mohamad *et al*., 2017; Fang *et al*., 2017; Huacai and Jincui, 2017).

Cadmium is a heavy metal which is frequently used in industrial processes, including: nickel-cadmium batteries, anticorrosive agents and pigments. Albeit cadmium containing products can be recycled for industrial applications, and most cadmium pollution incidents arise from incineration and dumping of cadmium waste (Järup 2003). In the recent years, cadmium has attracted high attention due to its toxicity behavior which may lead into various diseases such as bone damage, acute respiratory distress syndromes (ARDS) and kidney damage (Barbier *et al*., 2005).

In the present work, the performance of a fixed-bed IE process comprising a commercial Amberjet 1500H strong cation exchange resin was assayed for removing cadmium ions from synthetic

Corresponding Author: A.A. Swelam, Chemistry Department, Faculty of Science, Al-Azhar University, Cairo, Egypt.
E-mail: abdelsamihswelam@yahoo.com

and natural wastewater. The effect of the concentration of cadmium ions, resin dose, temperature, the solution acidity and organic and inorganic salts was investigated. Moreover, the equilibrium behavior of this pollutant has been predicted by Langmuir, Freundlich, Temkin and D-R isotherms. Additionally, kinetics of cadmium ion adsorption on this resin has been investigated using pseudo-first order, pseudo-second order, Boyd and intraparticle diffusion models. Finally, the suitability of the proposed IE process.

Experimental:

Materials:

Analytical grade reagents and chemicals with purity over 99% were used for the analytical procedures, applied at least in triplicate.

Resin:

A strong-acid cation exchange resin Amberjet 1500H with sulphonic acid (SO_3H) group was used in this work.

Table 1: Physico-chemical properties of Amberjet 1500H strong cation exchange resin used.

Resins	AMBERJET 1500H
Physical form	Dark amber beads
Matrix	Styrene divinylbenzene copolymer
Functional group	Sulfonates acid
Ionic form as shipped	H^+
Total exchange capacity	≥ 2.00 eq/L (H^+ form)
Moisture holding capacity	45 to 51 % (H^+ form)
Shipping weight	820 g/L
Uniformity coefficient	≤ 1.20
Harmonic mean size	650 ± 50 µ m
Fine contents	< 0.425 mm :0.5 % max
Maximum reversible swelling	$Na^+ \rightarrow H^+$ < 10 %

Cadmium ion exchange experiments:

To evaluate the effect of the initial cadmium concentration. Ion exchange experiments were carried out during different batch operating periods. The effect of different initial concentrations of cadmium ion was examined. On the other hand, adsorption isotherm studies were carried out with different solution temperatures ranged from 298 to 318 K at 50 ml of a constant initial cadmium concentrations/resin dosage (0.5 g). Resulting data was fitted according to the following isotherm models: Langmuir, Freundlich, Temkin and D-R. Also, for the determination of the kinetics at the previous described conditions, data were fitted to the following kinetic models: first-order kinetic model, second-order kinetic models beside film and intraparticle diffusion models.

With the aim of obtaining the corresponding parameters for cadmium/H^+ equilibrium. Aqueous solutions of the contaminant were put in contact with the resin until equilibrium was achieved. The extent of the ion exchange equilibrium data of this pollutant was determined by measuring the residual amount of cadmium in the liquid phase. The flask containing the feed solution was stirred continuously during the whole experiment. The shaking rate and temperature were fixed at 150 rpm and room temperature (298 K), respectively, since these were the optimum values obtained in previous studies. Furthermore, the contact time was 240 min in order to ensure equilibrium conditions. The initial pH of the solution was neutral to the optimum value (pH≈7.0) found in former batch ion exchange experiments.

The amount of the adsorbed cadmium ions (q_e) in mg/g and their removal percentage of the aqueous solution was expressed according to the following equations:

$q_e = V(C_o - C_e)/m \times 1000$ (1)
Adsorption (%) = [(C0 -Ce)/C0]x100 (2)

where C_0 and C_e are the initial concentration and the concentration at equilibrium of Cd (II), in mg/l, respectively, m is the mass of the adsorbent and V is the volume of the solution (ml).

Adsorption kinetics of the metal ions.

To analyze the kinetics of the sorption process, four different reaction kinetic models were applied to determine the reaction order and rate constant of the cation exchange resin.

Pseudo-first order rate equation of Lagergren, 1898

The pseudo-first order equation of Lagergren is generally expressed as follows:

$$\frac{dq}{dt} = k_1(q_e - q_t) \quad (3)$$

where q_e and q_t are the amount of metal sorbed per unit weight of sorbent at equilibrium and at any time t, respectively (mg/g) and k_1 is the rate constant of pseudo-first order sorption (min^{-1}). After integration and applying boundary conditions, for $t = 0$, $q = 0$, the integrated form of Eq. (3) becomes

$$\ln(q_e - q_t) = \ln q_{e,1,\text{cal}} - k_1 t \quad (4)$$

The values of rate constant (k_1) and equilibrium capacity ($q_{e,1,\text{cal}}$) can be obtained from the slope and intercept of plotting log ($q_e - q_t$) against time for three temperatures.

The pseudo-second order equation

If the rate of sorption is a second order mechanism, the pseudo-second order chemisorption kinetic rate equation is expressed as (Ho, 2000)

$$\frac{dq}{dt} = k_2(q_e - q_t)^2 \quad (5)$$

where k_2 is the rate constant of pseudo-second order sorption (gm $mmol^{-1}$ min^{-1}), q_e is the amount of soluted sorbate at equilibrium (mg/g) and q_t is the amount of soluted sorbate on the surface of the resin at any time t (mg/g).

Integrating this equation (5) for the boundary conditions for $t = 0$, $q = 0$ gives

$$\frac{t}{q} = \frac{1}{k_2 q_{e,2}^2} + \frac{1}{q_{e,2}} t \quad (6)$$

and

$$h = k_2 q_{e,2}^2 \quad (7)$$

where h (mg g^{-1} min^{-1}) means the initial adsorption rate, and the constants can be determined experimentally by plotting of t/q against t.

Intra-particle diffusion model

The initial rate of the intraparticle diffusion is the following:

$$q_t = K_i t^{0.5} + C \quad (8)$$

where K_i is the intraparticle diffusion rate coefficient (mg $g^{-1}min^{-0.5}$) and C (mg g^{-1}) provides an idea about the thickness of the boundary layer **(**Weber and Morris, 1963). The K_i and C can be obtained from the slope and intercept of a straight line plot of q_t versus $t^{0.5}$.

Adsorption isotherm of the cadmium ions:

Adsorption isotherm experiments were also performed by agitating 0.5 g of the resin with a 50.0 ml aqueous solution of varying temperatures of the metal ion solution from 25 to 45 °C at a constant metal ion concentration of 674 mg/l. The contents were continually agitated in a temperature controlled flask shaker. At the end of the pre-determined time intervals. The amount adsorbed was determined from the difference in the initial and residual concentrations of the metal ion in the liquid phase. The data was fitted into the following isotherms:

Freundlich Adsorption Isotherm:

The Freundlich isotherm (Freundlich, 1906) is derived by assuming a heterogeneous surface with a non-uniform distribution of heat of sorption over the surface. It can be stated in the linear form as follows:

$$\ln q_e = \ln K_F + \frac{1}{n}\ln C_e \quad (9)$$

where K_F (mg g^{-1}) and n are isotherm constants indicate the capacity and intensity of the adsorption, respectively.

Langmuir Adsorption Isotherm

The Langmuir equation (Langmuir, 1918) is represented in the linear form as follows:

$$\frac{C_e}{q_e} = \frac{1}{K_L Q_{max}} + \frac{C_e}{Q_{max}} \quad (10)$$

Where C_e is the equilibrium concentration of adsorbate (mg/l), q_e is the amount of soluted sorbate at equilibrium (mg/l), K_L is the Langmuir adsorption constant (L $mmol^{-1}$) and Q_{max} is the theoretical maximum adsorption capacity (mg/g). Langmuir plots $\left(\frac{C_e}{q_e}\ vs.\ C_e\right)$ for adsorption of metal ions onto resins at different temperatures.

For the Langmuir isotherm model, a dimensionless constant (R_L), commonly known as separation factor or equilibrium parameter can be used to describe the favorability of adsorption on the polymer surface by:

$$R_L = \frac{1}{1+K_L C_0} \quad (11)$$

where C_0 is the initial metal ions concentration and K_L is the Langmuir equilibrium constant.

The Temkin Isotherm

The Temkin isotherm (Temkin and. Pyzhev, 1940) has been used in the following form:

$$q_e = \left(\frac{RT}{b_T}\right)\ln A_T + \left(\frac{RT}{b_T}\right)\ln C_e \quad (12)$$

Where $B_T = \left(\frac{RT}{b_T}\right)$, B_T is the Temkin constant (J/mol) related to adsorption heat, T is the absolute temperature (K), R is the gas constant (8.314 J/mol K), and A_T is the Temkin isotherm constant (L/g). (B_T) and (A_T) can be calculated from the slopes (b_T) and intercepts $(b_T \ln A_T)$ of the plot of q_e vs. $\ln C_e$.

Dubinin–Radushkevich isotherm model

The linear form of Dubinin and RadushKevich isotherm equation (Dubinin, and. Radushkevich, 1947) can be expressed as:

$$\ln q_e = \ln(X_{D-R}) - \beta\varepsilon^2 \quad (13)$$

where X_{D-R} is the theoretical monolayer saturation capacity (mg g^{-1}), β is the Dubinin–Radushkevich model constant ($mol^2\ J^{-2}$). ε is the polanyi potential and is equal to

$$\varepsilon = RT\ln\left(1+\frac{1}{C_e}\right) \quad (14)$$

where R, T and C_e represent the gas constant (8.314 J/mol K), absolute temperature (K) and adsorbate equilibrium concentration (mgl/L), respectively.

The X_{D-R} and β can be calculated from the slopes (β) and intercepts $\ln(X_{D-R})$ of the plot of $(ln\ q_e)$ vs. (ε^2) at different temperatures for metal ions onto the resins.

The value of E_{D-R} is related to the sorption mean free energy (KJ/mol). The relationship is expressed as:

$$E_{D-R} = \frac{1}{\sqrt{-2\beta}} \quad (15)$$

Adsorption thermodynamics:

The sorption data obtained from the above study (i.e. Effect of system temperature of sorption process) was used to calculate the thermodynamic parameters. The calculated Gibbs free energy change (ΔG), enthalpy change (ΔH) and entropy change (ΔS) values for the sorption process of metal ions by the three resins.

The Gibbs free energy change, ΔG (kJ/mol) was calculated from the following equation;

$$\Delta G = -RT \ln K_d \quad (16)$$

where R is the universal gas constant (8.314 J mol^{-1} K^{-1}), T is the absolute temperature (K) and K_d is the distribution coefficient of the adsorbate.

The relation between ΔG (kJ mol^{-1}), ΔH (kJ mol^{-1}) and ΔS (kJ mol^{-1} K^{-1}) can be expressed by the following equation;

$$\Delta G = \Delta H - T\Delta S \quad (17)$$

Combination of Eqs. (16) and (17) gives the van't Hoff equation (20):

$$\ln K_d = \frac{\Delta S}{R} - \frac{\Delta H}{RT} \quad (18)$$

The values of ΔH and ΔS were obtained from the slope $\left(\frac{-\Delta H}{R}\right)$ and intercept $\left(\frac{\Delta S}{R}\right)$, respectively, of the plot of $\ln K_d$ vs. $\frac{1}{T}$.

In order to further support the assertion that physical adsorption is the predominant mechanism, the values of the activation energy (E_a) and sticking probability (S^*) were estimated from the experimental data. They were calculated using a modified Arrhenius type equation related to surface coverage (θ) (Singh and Das, 2013) as expressed in equations:

$$\theta = 1 - \frac{C_e}{C_0} \quad (19)$$

where C_0 and C_e are the initial and equilibrium metal ion concentrations, respectively

$$S^* = (1 - \theta)\, exp\left(\frac{E_a}{RT}\right) \quad (20)$$

The sticking probability, *S**, is a function of the adsorbate/adsorbent system under consideration and is dependent on the temperature of the system.

The combination of Eqs. (19) and (20) gives the equation (21):

$$\ln \frac{C_e}{C_0} = \ln S^* + \frac{E_a}{RT} \quad (21)$$

The values of E_a and S^* were obtained from the slope $\left(\frac{E_a}{R}\right)$ and intercept $\ln S^*$, respectively, of the plot of $\ln \frac{C_e}{C_0}$ vs. $\frac{1}{T}$.

Results and Discussion

Distribution coefficients:

The distribution coefficients (K_d=C_e/q_e) for cadmium ions were determined by batch method. 0.5 g of each Amberjet 1500H in H^+ form was kept in 50 mL of 674 mg/l cadmium ion solutions at 25 °C ± 1 °C for 4 h, with intermittent shaking to reach equilibrium. The ion-exchange properties of the resin were studied by measuring the distribution coefficients (K_d) of cadmium ions using batch experiments in pure water. In addition to the nature of the ion exchange resin, various factors such as swelling, formation of complexes, nature of the chemical bond and solvent distribution may be responsible for the wide variation in the distribution coefficient values (Yavari *et al*., 2009). The obtained values for K_d (Fig.1) show that the resin is a useful ion exchanger.

Effect of the Cd(II) initial concentration:

The effect of the cadmium concentration on the ion exchange removal efficiency as well as on the amount of adsorbed cadmium per unit mass of resin is plotted in (Fig. 2). To carry out this study Cd (II) concentration was varied between 134 mg/ and 1489 mg/l and the cation exchange resin dosage was kept at 0.5 g/50ml.

Results showed that Cd (II) ions sorption onto the resin is strongly influenced by its concentration in the batch solution. It was obtained that the adsorption of Cd (II) onto Amberjet 1500H increases as Cd (II) concentration increased, from 12.6 mg/g for 134 mg/l initial iron concentration, to 123.09 mg/g for 1489 mg/l Cd (II) in the solution. On contrary, the adsorption percentage was decreases from 94.03 to 82.666%, as initial cadmium increase. This was due to the adsorbent of adsorption site is not saturated at low concentration. Additionally, this was due to the

increase in the driving force of the concentration gradient (Nguyen and Pho, 2014). These results confirmed that initial Cd (II) concentration played an important role in the adsorption.

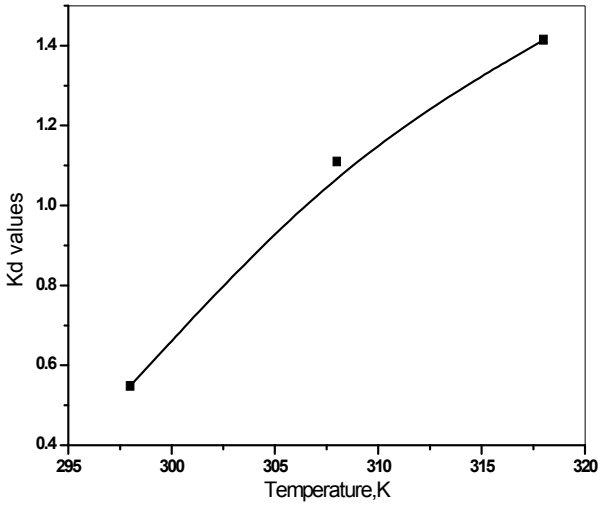

Fig. 1: Distribution ratio of Cd(II) in aqueous solution at different temperatures

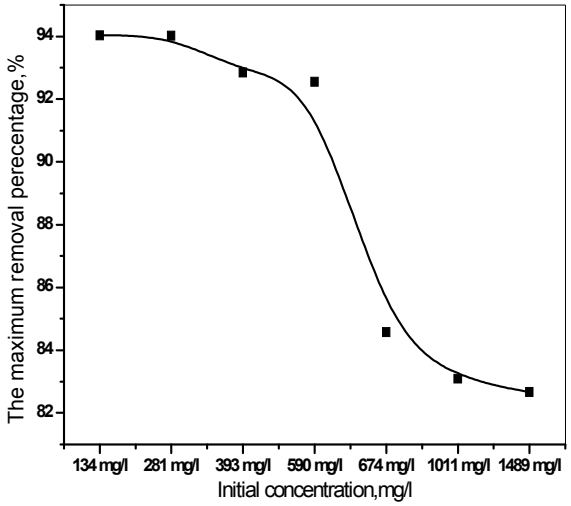

Fig. 2: Effect of Cd(II) concentration on the removal percentage

Effects of adsorption time and temperature on the adsorption capacity:

The effects of adsorption time and temperature on the adsorption of Cd(II) were reflected in (Fig. 3). It could be seen that the adsorption rate is fast from 0 min to 60 min. With the increasing of time, the adsorption rate slowed down. The adsorption equilibrium could be reached within 240 min at 298K and 180 at both 308 and 318K. In the initial stage of adsorption process, there are a large number of adsorption sites on the resin. Many Cd(II) could be assembled onto the resin material and result in Cd(II) adsorption quantity rising faster. With the increasing of time, the adsorption sites were decreased, and the adsorption rate slowed down gradually to reach the adsorption equilibrium. At the same time,(Fig. 3) showed that the different temperature had great influence on the adsorption quantity of Cd(II) on the resin. With the increasing of temperature, the adsorption of Cd(II) presented a trend of increasing.

When the temperature is 318 K, the adsorption of Cd(II) is the largest, indicating endothermic nature of the adsorption process. This could be due to activation and faster movement of Cd(II) toward the coordinating sites of adsorbent, Amberjet 1500H, at high temperature (Kosa *et al*., 2012). Low temperature is not conducive to the adsorption process.

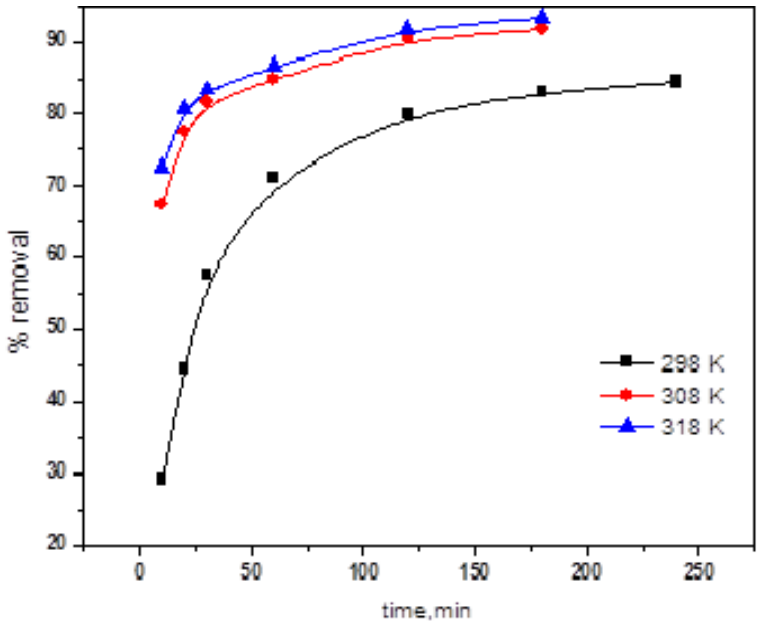

Fig. 3: Effect of the temperature on the Cd (II) uptake (%)

Effect of solution acidity:

The effect of solution acidity on Cd (II) removal was investigated in the hydrochloric acid concentration ranges of 0.005–3.0 M at 298 K for 4 h as shown in (Fig. 4). The extractability of the cations from the solution phase is pH dependent because of its effect on the solubility of the metal ions, concentration of the counter ions on the functional groups of the adsorbent and the degree of ionization of the adsorbate during reaction (Kazutoshi and Takashi 2012). From the corresponding data, an increase in acid concentration corresponded to decrease in adsorption capacity, reaching the minimum adsorption rate at 3.0 M. At the higher acid concentration (>2.0 M) there was nearly no adsorption of Cd (II). With the acid concentration increasing, the Cd (II) adsorbed decreased from 81.602% to 10.85%. On lowering solution acidity values obvious an increase of adsorption for Cd (II) was observed. Cd (II) could be suffering hydrolysis and different species was formed $(Cd(OH))^{+}$ in addition to Cd^{2+} which promotes an increase of the adsorption capacity. The results indicated that the solution acidity remarkably impacted on the adsorption of Cd (II) onto the Amberjet 1500H resin.

Effect of resin dosage:

The resin dosage of 0.25, 0.5, 1.5, 3.0, 5.0, 8.0 and 10 g were used in 674 mg/l Cd (II) solutions under neutral solution to test their effects on Cd (II) adsorption. As shown in (Fig. 5), the adsorption effective of Cd (II) by Amberjet 1500H resin with increases in the resin dosage from 71.958% to 91.661%. When resin dosage was above 1.5 g, the adsorption effective was decreased to reach 42.196%. However, reverse trend was observed with adsorbed Cd (II) by unit amount of resin which decreased from 97 mg/g at resin dose of 0.25 g to 4.74 mg/g at resin dose of 3.0 g. Once the interaction of Cd (II)-resin reached equilibrium, the addition of extra adsorbent was probably left unutilized or unsaturated. These unutilized masses of resin were accounted however during the calculation of removal capacity, leading to reduction of q_e value (Shek *et al*., 2009; Mayesa *et al*., 2009). It suggested that the most economic resin dosage was 10 g in 1 L solutions to treat wastewater with Cd (II) of 674 mg/l.

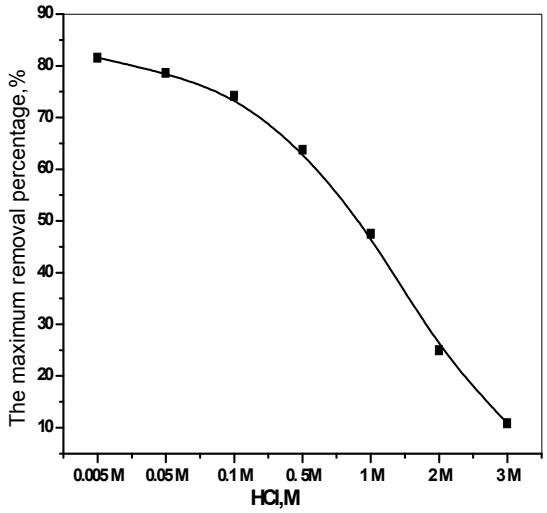

Fig.4: Effect of HCl concentration on the removal percentage of Cd(II) from aqueous solution

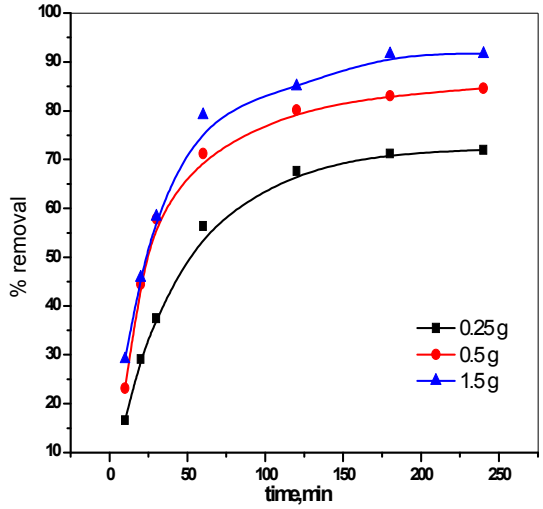

Fig.5: Effect the resin dose on the removal percentage of Cd(II) from aqueous solution

Effect of Ionic strength:

Effect of NaCl and/or $NaNO_3$ solutions on the metal uptake:

The influence of ionic strength on adsorption of cadmium (II) onto the resin was described in (Fig. 6). Apparently, the existence of NaCl or $NaNO_3$ generally inhibit the adsorption of Cd (II) and decreased obviously. Moreover, the inhibition of adsorption capacity of Cd (II) ranked as: 1.0 M > 0.1 M > 0.05 M. Generally, ionic strength basically behave in the following ways: (1) changing the structure of double electrode layer of the adsorbent; (2) reducing the radius of hydrated ions; (3) competing the activity sites with metal ions (Ting *et al*., 2013). For Cd (II) in this process, the third way could be primary, while the other two were secondary. The existence of Na^+ may cause steric hindrance to Cd (II) due to their larger radius leading to the reduction of Cd (II) adsorption capacity. The stronger ionic strength brought more occupied active sites by Na^+, and the lower adsorption capacities of Cd (II) were.

Effect of acetate and citrate solutions on the metal uptake:

The examination of the influence of acetate and citrate at various concentrations (0.05 – 1.0M for each) on the position of the equilibrium of Cd(II)-resin interactions are shown in (Fig. 7). As can be seen from the (Fig.7) that the amount of the metal ions, q_e, taken up by the resin sample decreases with increasing concentration of both acetate and citrate solutions. This may be explained in terms of the steric hindrance and the higher stability constants of the complexes formed by the metal ion with the two electrolytes used in the present study. Comparing with acetate and citrate more significantly inhibited Cd (II) adsorption, suggest the order of adsorption capacity of the cadmium complexes, is citrate < acetate complexes. The sizes of the ligands are in the following order; the acetate ($C_2H_3O_2^-$) is the smallest than that of citrate ($C_6H_7O_7^-$). It is therefore likely that the size of the ligands played important role in the order of the metal complex adsorption, where the adsorption capacity of the calcium and magnesium complexes was influenced by the steric hindrance or the crowding effect associated with the comparative bulkiness of the organic ligands in the metal complexes. Generally, the metal ion forms a complex with the acetate ion and the sorption depends upon the nature of complex formed (Ho and Mckay 1998). As the concentration of acetate is increased, acetate ion replaces the coordinating water molecule resulting in the formation of complex species of a small positive charge, and consequently qe is lowered. A further increase in the concentration of acetate leads to the formation of a neutral species and this also results in decrease of qe. When the concentration of acetate is higher and a neutral metal acetate is likely to be present in solution, the

predominant species in the resin phase would be $M^{2+}(OAc)^{+}$ or $M^{3+}(OAc)^{2+}$ as inferred by workers (Ho 2006; Zeldowitsch, 1934).

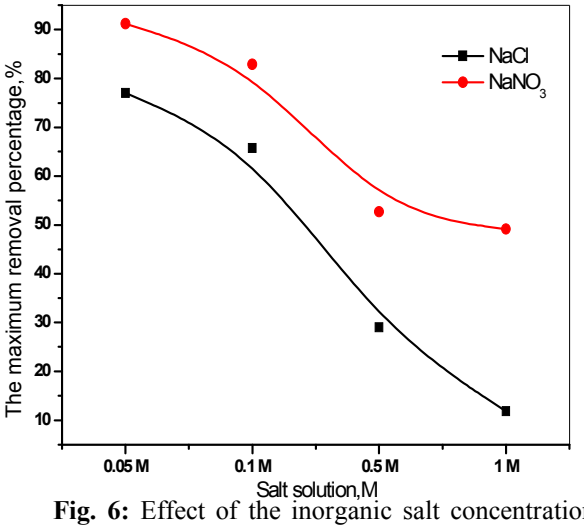

Fig. 6: Effect of the inorganic salt concentrations on the Cd(II) uptake (%)

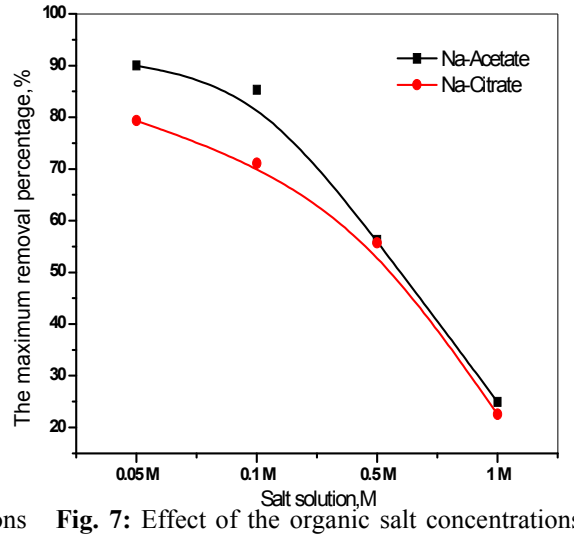

Fig. 7: Effect of the organic salt concentrations on the Cd(II) uptake (%)

Equilibrium isotherms:

The experimental data at equilibrium amount of adsorbed Cd (II) on Amberjet 1500H (q_e) and the concentration of Cd (II) in the liquid phase (C_e) at different temperatures were used to describe the optimum isotherm model. The linear forms of Langmuir, Freundlich, Temkin and D-R equations were used to describe the equilibrium data. The performance of each form was judged through the correlation coefficients (R^2).

Ion exchange resin, after coming in contact with the solution, exchanges counter ions and attain equilibrium. The exchange is reversible in nature and the concentration ratio of both ions might not be the same in the two phases, i.e. resin and solution phase (Helfferich, 1962). The description of the equilibrium in the ion exchange system is usually made by equilibrium isotherms, which represent the distribution of the adsorbed solute in the resin ($Cd_{adsorbed}$) and the free solute in the fluid phase ($Cd_{solution}$), in equilibrium.

The ion exchange reaction of the cadmium system using the cationic resin Amberjet 1500H can be represented by:

$$CdCl_2+2R–H \rightleftarrows 2R–Cd +2HCl \quad (22)$$

When cadmium solution takes contact with Amberjet 1500H, the resin fixes cadmium ions and releases hydrogen protons.

Adsorption isotherms play a crucial role in the predictive modelling procedures for the analysis and design of adsorption systems, which are essential for real-scale operation (Ould Brahim *et al*., 2014).

Freundlich isotherm model is an empirical relationship describing the ion exchange of solutes from a liquid phase to a solid surface, which assumes that different sites with several uptake energies are involved (Freundlich, 1906). It is commonly used to describe the adsorption characteristics for heterogeneous surfaces. Freundlich isotherm represents the relationship between the amounts of ionic species exchanged per unit mass of resin, q_e, and the concentration of the ionic species at equilibrium, C_e.

Langmuir isotherm model is employed to predict the ion exchange of aqueous compounds onto a solid phase (Langmuir, 1918). This mechanistic model accepts that a monolayer of adsorbed material is adsorbed over a uniform adsorbent surface (a flat surface of solid phase) at a constant temperature, and that the distribution of the compound between the two phases is controlled by the equilibrium

constant. Hence, under equilibrium conditions rates corresponding to adsorption and desorption processes should be equal.

Also, Temkin isotherm model was finally tested to model the adsorption potential of Amberjet 1500H resin towards cadmium. This model takes into account the effects of indirect adsorbent (resin)/adsorbate (cadmium) interactions on the adsorption process (Temkin and Pyzhev, 1940).

The isotherm experimental data as well as the fit to the four tested isotherm models are studied. The relevant coefficients of each model and the calculated linear fit means squares are also reported in (Table. 2).

Table 2: Langmuir, Freundlich and Temkin isotherm parameters for cadmium ions uptake on Amberjet 1500H resin.

Freundlich			Langmiur			
n	K_f (mg/g)	R^2	Q_{max} (mg/g)	K_L (L/mg)	R_L	R^2
8.26	100.12	0.9879	52.91	0.1321	0.01136	0.9996
Temkin			Dubinin Redushkevich (D-R)			
A_T (L/g)	B_T (J/mol)	R^2	B mol^2/J^2	X_m (mg/g)	E (kJ/mol)	R^2
3.63×10^{-6}	7.24	0.9901	3.57×10^{-5}	56.35	118.36	0.8131

The value of the *n* coefficient is higher than 1(8.26), which highlights the favorability of the adsorption process. It can be seen that the R^2 values obtained from the Freundlich model did not show a consistent trend and also the experimental q_e ($q_{e\ exp}$) values did not agree with the calculated values ($q_{e\ cal}$) obtained from the linear plot (Fig. not shown). This shows that adsorption of the metal ion onto the resin does not follow a Freundlich model.

For Langmuir isotherm, the adsorption of cadmium onto Amberjet 1500H resin is described by means of q_{max}, K_L and R^2 values. The results indicate that the linear form of Langmuir model fits well with experimental data, as indicated by the high value of the regression coefficient ($R^2 > 0.999$) (Fig. not shown). On the other hand, the maximum ion exchange capacity, q_{max}, was calculated as 52.91 mg g^{-1} (Table 2).

In this case, the R_L value was 0.01136, which is less than unity, for cadmium temperatures ranging 298-318 K. These R_L values indicate that the adsorption of cadmium ions onto Amberjet 1500H cation exchange resin is a favorable process, and the data fit accurately the Langmuir isotherm model.

The monolayer adsorption capacity (Q_{max}) values of 52.91 mg/g for Cd (II) observed in this study compared well with some other adsorbents reported from literature such as 5.41 mg/g from dolomite powder (Mohammadi *et al*., 2015), 42.41 mg/g by modified chitosan (Cheng *et al*., 2014), 44.44 mg/g from *Bacillus laterosporus* MTC C 1628 Kulkarni and Shetty, 2014). 70.92 mg/g by modified plantain peels (Zaharaddeen *et al*., 2016).

On the other hand, the A_T and B_T parameters of the Temkin equation were calculated for cadmium ions adsorption (Table 2). It was obtained that the value of R^2 for Temkin model (0.9901) is higher than that calculated for Freundlich model (0.9879). The data of equilibrium isotherms for the system cadmium/Amberjet 1500H is better described by the Temkin model as it can be observed.

Dubinin–Radushkevich (D–R) isotherm:

Dubinin–Radushkevich isotherm assumes a fixed volume or 'sorption space' close to the sorbent surface and determines the heterogeneity of sorption energies within the sorption space and is applied in the linearized form. The plot of ln q_e versus ε^2 yield coefficients of determinations and the result of X_m (56.35) computed from the slope and intercept of respective plots are documented in Table 2. R^2 values (0.8131) showed that the D–R model poor fit to the experimental data of cadmium adsorption. The mean free energy of sorption (E) can be defined as the free energy change when one mole of ion is transferred from infinity in solution to the sorbent. The E value in our study show a low value (118.36 kJ mol^{-1}), indicating the chemical nature of the cadmium adsorption processes onto the resin.

It is shown from the above discussion that the experimental data of Cd (II) adsorption processes on the Amberjet 1500H could be fitted by the isotherms. The fitting order of the different adsorption models according to R^2 values was as follows; Langmuir (0.9996) > Temkin (0.9901) > Freundlich (0.9879) > D – R (0.8131). Clearly, the Langmuir equation provided better fitting in terms of R^2 values (0.9996).

Ion Exchange kinetics:

In order to study the adsorption rate of cadmium on the selected strong-acid cation exchange resin, experimental data obtained at several temperatures were fitted to different kinetic models. Namely the pseudo-first-order, the pseudo-second order, intraparticle diffusion and film diffusion models were tested. The reliability of these kinetic models was determined by measuring the coefficients of determination (R^2).

Finally, in order to investigate any possible mechanisms of Cd (II) adsorption onto Amberjet 1500H, intra-particle diffusion and film diffusion-based mechanism was also studied. According to these model, the uptake of the adsorbate by the adsorbent varies almost proportionately with the square root of the contact time ($t^{1/2}$). Weber and Morris (1962) proposed the most widely applied intra-particle diffusion equation for sorption systems. The rate parameter k_i of stage i is obtained from the slope of the straight line resulting of plotting q_t vs. $t^{1/2}$.

The results of the fit of the experimental ion exchange data to the different tested kinetic models are hereafter summarized in Table 3 and Table 4. The values for parameters obtained after application of the kinetic models were used to predict the variation of adsorbed Cd (II) ions with time.

Table 3: Kinetic parameters for Cd(II) adsorption in aqueous media.

	Pseudo first-order model			Pseudo second-order model			
Temp, K	$qe_{,1,}cal$	K_1	R^2	$qe_{,2,}cal$	K_2	R^2	h
	mg/g	min^{-1}		mg/g	(g/mgmin)		
298	37.92	0.0207	0.9863	61.96	0.00083	0.9995	3.20
308	17.59	0.0253	0.9725	63.29	0.00345	0.9998	13.83
318	14.98	0.0223	0.9742	64.14	0.00384	0.9997	15.81

For the first-order kinetics model, the values of k_1 and q_e were calculated from the slope and the intercept of the plots of log ($q_e - q_t$) vs. t, respectively, at different concentrations. The results summarized in Table 3 show that the values of R^2 (0.9742) are relatively low and the experimental q_e values do not agree well with the calculated values. This reveals that the adsorption of Cd (II) onto Amberjet 1500H resin does not follow first-order kinetics.Otherwise, the value of q_e and k_2 could be calculated from the slope and intercept of the plot of t/q_t vs. t, respectively. The results plotted show linear plots for all the assayed temperatures, with very high values of R^2 (0.9997) in addition to the good agreement between the experimental and calculated values of q_e (Table 3). Therefore, the adsorption rate of cadmium onto the resin fits with utmost accuracy the pseudo second-order kinetics. On the other hand, if the intraparticle diffusion is the controlling mechanism of the adsorption process, then the plot of q_t vs. $t^{1/2}$ should be linear, and if it passes through the origin, the rate limiting process is only due to the intraparticle diffusion (Elmorsi, 2011).

The results of the fit of the experimental data to the intraparticle diffusion model was reported for the studied feed concentrations range. The results indicate that the plots of qt vs. $t^{1/2}$ are not linear over the whole operating time. Furthermore, it can be seen that the intraparticle diffusion of cadmium occurred in two sequential stages: the first straight portion is attributed to the macrospore diffusion whereas the second linear portion might be mainly related to microspore diffusion (Weber and Morris, 1962). Such finding is supported by former results obtained in previous works on metal ions adsorption by Elmorsi 2011. In addition, the sorption rate was generally fast and the intraparticle

diffusion was not found to be the rate-limiting step (Table 4) which occurred in the same way in case of sorption of other metal ions (Prasad and Saxena, 2004).

Boyd kinetic model:

The third step in the adsorption dynamics of Cd (II) ion is assumed to be very rapid and it can be considered negligible. For design purposes, it is required to distinguish between film diffusion and particle diffusion of adsorbate molecules. In order to identify the slowest step in the adsorption process, Boyd kinetic equation (Boyd *et al*., 1947) was applied, which is expressed as:

$$F = 1 - \frac{6}{\pi^2}\exp(-Bt) \tag{23}$$

$$F = \frac{q_t}{q_e} \tag{24}$$

where q_e is the amount of Cadmium (II) adsorbed at equilibrium (mg/g) and q_t represents the amount of cadmium (II) adsorbed at any time t, F represents the fraction of cadmium (II) adsorbed at any time t, and Bt is a mathematical function of F(Reichenberg, 1953).

The plot of Bt against time t can be employed to test the linearity of the experimental values. If the plots are linear and pass through the origin, then the slowest step in the adsorption process is the internal diffusion. From the result obtained, it was observed that the plots are linear, but do not pass through the origin, suggesting that the adsorption process is controlled by film diffusion. The calculated B values were used to calculate the effective diffusion coefficient, D_i (m^2/s) using the following relationship:

$$B = \frac{\pi^2 D_i}{r^2} \tag{25}$$

where D_i is the effective diffusion coefficient of Cd (II) in the Dowex HCR-S/S surface and r is the radius of the resin particles. The D_i values were found to be $1.77x10^{-4}$, $2.53x10^{-4}$ and $1.83x10^{-4}$ at 298, 308 and 318 K, respectively. A Boyd kinetic plot confirms that the external mass transfer was the slowest step involved in the adsorption process.

As it can be seen, we conclude the relative errors of the second-order model are lower than in other models, and the correlation coefficients of the second-order model were found to be higher, indicating that this model describes better the adsorption of Cd (II) on Amberjet 1500H. On the other hand, results indicate that the adsorption kinetic coefficients were dependent on the initial temperatures. Table 4 shows that the lowest differences between the theoretical $q_{e,\ cal}$ and the experimental $q_{e,\ exp}$ equilibrium adsorption capacity values are ensured by the second order rate equation. Nevertheless, the intraparticle diffusion and film diffusion equations also provide a good fitting of the experimental data points for the whole set of the tested initial concentrations. Considering all these results, the kinetics of iron adsorption on the selected strong-acid cation exchange resin could be satisfactorily described by both pseudo-second order and intraparticle diffusion model equations.

Table 4: Kinetic parameters for CdII) in aqueous media.

Temp, K	Intraparticle diffusion model			Film diffusion	
	Ki	C	R^2	Di	R^2
	(mg/g min) $^{0.5}$	(mg/g)		(cm2/s)	
298	2.80	19.07	0.8137	$1.77x10^{-4}$	0.98961
308	1.40	44.95	0.8062	$2.53x10^{-4}$	0.97577
318	1.22	48	0.8571	$1.83x10^{-4}$	0.97403

Thermodynamic Studies:

The positive ΔG^0 values (Table 5) at low temperatures (298 and 308K) indicate nonspontaneous of the adsorption processes at these temperatures while negative ΔG^0 value at higher temperature (318K) indicate the spontaneous process of Cd (II) adsorption. Under the reaction conditions. ΔG^0 becomes lower positive values to reach negative with increase of temperature, which indicated more efficient adsorption at high temperature. The energy related to the adsorption are usually measured from the changes in some of the thermodynamic parameters such as enthalpy ($\Delta H°$), and entropy ($\Delta S°$). In this research work, the thermodynamic parameters of the Cd (II) adsorption were studied at three different temperatures (298, 308 and 318 K). ΔH value was positive, showing that the sorption of Cd (II) was endothermic and Cd (II) ions were well solvated in aqueous solution at high temperature (Zhang *et al*., 2016). The removal of water molecules from ions is essentially an endothermic process, and apparently, the energy of dehydration exceeds exothermicity of Cd (II) to attach to the resin surface.

Table 5: Thermodynamic parameters in aqueous media.

Metal ions	T(K)	S*	ΔS^0	ΔH^0	ΔG^0	Ea
			j/mol K	kJ/mol	kJ/mol	kJ/mol
Cd (II)	298	2.20×10^{-7}	120.21	37.14	1.49	33.20
	308				-0.2674	
	318				-0.8898	

The positive $\Delta S°$ confirmed the randomness increased at the solid-solution interface during adsorption (Hamid *et al*., 2014). In addition, Cd (II) in solution was surrounded by a tightly bound hydration layer and water molecules were more highly ordered. When Cd (II) came into close interaction with the hydration surface of sorbent, the ordered water molecules in the two hydration layers were compelled and disturbed, thus increasing the entropy of water molecules. This was consistent with the results that Cd (II) adsorption at pH ≈ 7 is mainly dominated by cation exchange.

In order to further support the assertion that the adsorption is the predominant mechanism, the values of the activation energy (E_a) and sticking probability (S*) were estimated from the experimental data. They were calculated using a modified Arrhenius type equation related to surface coverage (Singh and Das 2013). The sticking probability, S*, is a function of the adsorbate/adsorbent system under consideration and is dependent on the temperature of the system. The parameter S* indicates the measure of the potential of an adsorbate to remain on the adsorbent indefinitely. It can be expressed as in Table 5. The effect of temperature on the sticking probability was evaluated throughout the temperature range from 298 to 318 K by calculating the surface coverage at the various temperatures. Table 5 also indicated that the values of $S^* \leq 1$ (2.20×10^{-7}) for the Amberjet 1500H, hence the sticking probability of the Cd (II) ion onto the two adsorbent systems are very high.

Sorption activation energy:

According to Arrhenius equation, activation energy of the adsorption (E_a, J mol^{-1}) can be calculated using the above equation. The magnitude of activation energy gives an idea about the type of adsorption which is mainly physical or chemical. Low activation energies (<40 kJ mol^{-1}) are characteristics for physical adsorption, while higher activation energies (>40 kJ mol^{-1}) suggest chemical adsorption (Anirudhan *et al*., 2008). According to activation energy obtained for the adsorption of cadmium onto the resin was 33.20 kJ mol^{-1} indicates that the adsorption process is physisorption. The low value of E_a suggests that the energetic barrier against the adsorption of metal ion is easy to overcome; therefore, adsorption process occurs rapidly (Sagnik *et al*., 2011).

Influences of co-existing cations:

For cation exchange, the co-existing cations may reduce the adsorption capacity via competing effect. Wastewater typically contains different many ions. Therefore, it is important to investigate the influence of co-existing cations on the adsorption of each other. Competitive adsorption of Pb(II),

Cu(II), Cd(II), Ni(II), Co(II) and Fe(III) by the Amberjet 1500H in synthetic single and multi-systems was studied. All metal ions removal performance of 0.5g the Amberjet 1500H cation exchange resin was evaluated as a function of 50 ml Pb(II), Fe(III), Cu(II), Cd(II), Ni(II) and Co(II) solution of constant initial ion concentration (ppm) for each. The metal ions were analyzed by flame atomic absorption spectrometry as above. In this study, the adsorption time was fixed at 300 min because the adsorption of the metal ion onto the Amberjet 1500H sufficiently reached an equilibrium state based on the contact time dependency test.

The maximum removal percentage (%):

To evaluate the effects of the co-existing cations, different mixtures (1-5) were shaken at 298 ± 1 K and 180 rpm for constant time interval 300 min (Table 6). The data shows the maximum removal capacity (%) of the each metal ion for five multi-systems, in addition to in single systems. As can be seen from The mixture 1, the maximum removal capacity (%) was in sequence of Cu(II) >Ni(II) > Cd(II) > Co(II) > Fe(III) >Pb(II) and Cu(II) > Cd(II) > Ni(II) > Fe(III) > Co(II) >Pb(II)from single and multi-systems, respectively. In The mixture 2, the sequence was Co(II) > Ni(II) > Cu(II) >Fe(III) >Pb(II) and Co(II) > Cu(II) > Ni(II) >Fe(III) >Pb(II) in single and multi-systems, respectively. However, in the mixture 3, the sequence was Ni(II) >Cd(II) >Cu(II) >Fe(III). On the other hand, in presence of 0.1M NaCl and $NaNO_3$, in mixtures 4 and 5, respectively, the maximum removal capacity (%) was in the sequence of Cd(II) > Pb(II) from single and multi-systems.

Table 6: The removal percentage of the metal ions in single and multi- systems

Mixture 1						
Metal ion	Cd(II)	Co(II)	Cu(II)	Ni(II)	Pb(II)	Fe(III)
C_0 (mg/l)	128.2	12.9	79.13	35.81	260	348
%, Single	98.58	96.12	99.50	98.91	91.66	94.26
%, Mixture	99.42	93.16	99.49	98.92	91.66	94.26
Mixture 2						
	Pb(II)	Co(II)	Cu(II)	Ni(II)	Fe(III)	
C_0 (mg/l)	337.8	18	67.82	39	312	
%, Single	91.01	99.67	97.29	99	95.35	
%, Mixture	91.01	99.68	97.29	96.98	95.35	
Mixture 3						
	Cd(II)	Cu(II)	Ni(II)	Fe(III)		
C_0 (mg/l)	123.80	62.39	26.18	365		
%, Single	98.53	97.05	98.93	93.10		
%, Mixture	98.53	97.52	98.95	93.15		
Mixture 4						
	Cd(II)	Pb(II)				
C_0 (mg/l)	118.8	250				
%, Single	98.49	91.32				
%, Mixture	92.05	89.0				
Mixture 5						
	Cd(II)	Pb(II)				
C_0 (mg/l)	121.6	86.87				
%, Single	98.52	98.27				
%, Mixture	90.06	90.01				

The distribution ratio:

The distribution ratio of each metal ion whether, in single or multi-systems was evaluated in different mixtures (1-5) at 298 ± 1 K and 180 rpm for constant time interval (300 min) using 0.5 g resin/50 ml solution, to study the effects of the co-existing cations on each other. The data (Table 7) shows the distribution ratio (K_d) of the each metal ion. As can be seen from the mixture 1, the K_d value was in sequence of Cu(II) > Ni(II) > Cd(II) > Co(II) > Fe(III) > Pb(II) and Cu(II) >Cd(II) > Ni(II) > Fe(III) Co(II) >Pb(II) in single and multi-systems, respectively. In the mixture 2, the

sequence was Co(II) > Ni(II) >Cu(II) >Fe(III) >Pb(II) and Co(II) > Cu(II) > Ni(II) >Fe(III) >Pb(II) in single and multi-systems respectively. However, in the mixture 3, the sequence was Ni(II) > Cd(II)> Cu(II) > Fe(III) in both single and multi-systems. On the other hand, in presence of 0.1M NaCl and $NaNO_3$, in the mixtures 4 and 5, respectively, the K_d value was in the sequence of Cd(II) > Pb(II) from single and multi-systems.

Table 7: The distribution ratio of the metal ions in single and multi-systems

Mixture 1						
Metal ion	Cd(II)	Co(II)	Cu(II)	Ni(II)	Pb(II)	Fe(III)
C_0 (mg/l)	128.2	12.9	79.13	35.81	260	348
Kd-Single	6.95	2.48	19.68	9.08	1.1	1.64
Kd-Mixture	17.23	1.36	19.54	9.17	1.1	1.64
Mixture 2						
	Pb(II)	Co(II)	Cu(II)	Ni(II)	Fe(III)	
C_0 (mg/l)	337	18	67.82	39	312	
Kd-Single	1.01	29.9	3.59	9.9	2.05	
Kd-Mixture	1.01	31.4	3.58	3.2	2.05	
Mixture 3						
	Cd(II)	Cu(II)	Ni(II)	Fe(III)		
C_0 (mg/l)	123.80	62.39	26.18	365		
Kd-Single	6.7	3.29	9.25	1.35		
Kd-Mixture	6.7	3.93	9.39	1.36		
Mixture 4						
	Cd(II)	Pb(II)				
C_0 (mg/l)	118.8	250				
Kd-Single	6.5	1.05				
Kd-Mixture	1.16	0.9				
Mixture 5						
	Cd(II)	Pb(II)				
C_0 (mg/l)	121.6	86.87				
Kd-Single	6.66	5.69				
Kd-Mixture	0.91	0.9				

The ratio q_e'/q_e:

Multi component adsorption studies are important to assess the degree of interference posed by common metal ions present in wastewaters. The sorption dynamics of the mixture was probed using qe′/qe ratios, were the prime denotes the presence of other metal ions. In general, five possible types of mixtures are exhibited in multicomponent adsorbates–adsorbent (Arup and Jayanta, 2013) $q_e'/q_e > 1$, synergism (the effect of the mixture is greater than that of the individual adsorbates in the mixture); qe′/qe <1, antagonism (the effect of the mixture is less than that of each of the individual adsorbate in the mixture) and qe′/qe=1, non-interaction (the mixture has no effect on the adsorption of each of the adsorbate in the mixture).

The multi-metal sorption ions in aqueous systems by Amberjet 1500H were investigated to establish the effect of the presence of different metal ions on the sorption of each one of them. The qe′/qe ratios for the sorption of one metal (Cd(II)) in the presence of other metals are shown in Table 8. The ratios of Cd(II) ion were > 1.0 indicated that, synergism (the effect of the mixture is greater than that of the individual adsorbates in the mixture) and =1.0, indicated that, non-interaction (the mixture has no effect on the adsorption of each of the adsorbate in the mixture) in mixtures 1 and 3, respectively. an opposite trend was observed in mixtures 4 and 5, which qe′/qe ratio was < 1.0, indicated that the adsorption of Cd(II) was depressed by the presence of Pb(II) ion and NaCl from one hand and by presence of Pb(II) and $NaNO_3$ from other hand in the tertiary solutions; hence the effect of the mixtures seemed to be antagonistic. The qe′/qe ratios for the sorption of Pb(II) ion in the presence of Cd(II), Cu (II), Ni(II), Co(II) and Fe(III) (mixture 1) was equal to unity and, indicated that, non-interaction (the mixture has no effect on the adsorption of each of the adsorbate in the mixture). On the other hand, qe′/qe ratio was < 1.0 in the mixtures 2,4 and 5, indicated that the adsorption of the Pb(II)

was depressed by the presence of Co(II), Cu(II), Ni(II) and Fe(III) ions, in presence of Cd(II) and NaCl from one hand and by presence of Cd(II) and $NaNO_3$ from other hand in the tertiary solutions; hence the effect of the mixtures seemed to be antagonistic.

Table 8: The q_{eMix} /$q_{eSingle}$ ratio

Mixture 1						
Metal ion	Cd(II)	Co(II)	Cu(II)	Ni(II)	Pb(II)	Fe(III)
C_0 (mg/l)	128.2	12.9	79.13	35.81	260	348
q_{eMix} /$q_{eSingle}$	1.008703	0.967742	1.000381	0.999435	1.0000	1.000
Mixture 2						
	Pb(II)	Co(II)	Cu(II)	Ni(II)	Fe(III)	
C_0 (mg/l)	337	18	67.82	39	312	
q_{eMix} /$q_{eSingle}$	0.999967	0.99777	0.999848	0.979275	1.00	
Mixture 3						
	Cd(II)	Cu(II)	Ni(II)	Fe(III)		
C_0 (mg/l)	123.80	62.39	26.180	365.0		
q_{eMix} /$q_{eSingle}$	1.0000	1.004959	1.000154	1.000589		
Mixture 4						
	Cd(II)	Pb(II)				
C_0 (mg/l)	118.8	250				
q_{eMix} /$q_{eSingle}$	0.934188	0.985545				
Mixture 5						
	Cd(II)	Pb(II)				
C_0 (mg/l)	121.6	86.87				
q_{eMix} /$q_{eSingle}$	0.914023	0.915691				

This value indicates that there was a significant difference in the magnitude of suppression of lead ion uptake in the presence of other metal ions and, NaCl and $NaNO_3$. Thus, these results show that in all cases, there was an inhibitory effect of one metal on binding of the other metal. Interestingly, the overall adsorption capacities of the Amberjet 1500H for Pb(II) in the multi-systems were lower than the adsorption capacities of Pb(II) in the single component systems. For that reason, the adsorption sites of Pb(II) ion may partially be overlapped with the other ions in multi-systems.

Real wastewater treatment:

Upon completion of basic adsorption tests, effluent of a local industrial plant, surface and ground waters were treated by the Amberjet 1500H The metal concentration of the collected wastewater was measured at the beginning of adsorption tests, are presented in Table 9. For this, a bulk wastewater sample was collected at winter (January 2017) from local Industrial wastewater (Battery Factory-Zone of Abu Rawwash-area-El Giza), Surface water (Canal-Anani village-Monouf-El Monofia), lake (Lake oxidative-Sadat City-El Monofia) and groundwater (Groundwater-El Tahadi Road-El Nagah village-El Bohira). Adsorption was performed with 100 ml of contaminated water with Amberjet 1500H dose of 1 g. The suspensions were stirred at a room temperature (20 °C) and 150 rpm.

Table 9: Distribution of the different contaminated water sources

Sample No.	The contaminated water source
S1	Industrial wastewater-Battery Factory-Zone of Abu Rawwash-area-El Giza
S2	Surface water-Canal-Anani village-Monouf-El Monofia
S3	Surface water-Lake oxidative-Sadat City-El Monofia
S4	Groundwater-El Tahadi street-El Nagah village- El Bohira

The results in Fig.8 showed that the metal uptake (mg/g) for Zn(II) in S4 > S3 > S1 > S2 and for Pb(II), the metal uptake (mg/g) in S3 > S1> S4 > S2, while the metal uptake (mg/g) of Cd(II) in S3 > S4 > S2 > S1, respectively, which are significantly different from each other.

The low value of metal ion uptake in surface water may be due to the retardation effects of organic matter (humic substances) present in river water. Similar results were also reported by Lu *et al*., 2017who noted that soluble organic matter in natural water already present can form complexes

with cations, thus hindering heavy metal sorption. In addition, organic matter present in water could act as a inhibitors to retard the interaction of the metal ion (Rangel *et al*., 2009). On the other, the low value of the metal ion uptake in S1 and S4 samples, it can be attributed to the competition for adsorption sites by solids and other interfering ions which already present in the water samples (Dinesh *et al*., 2014).

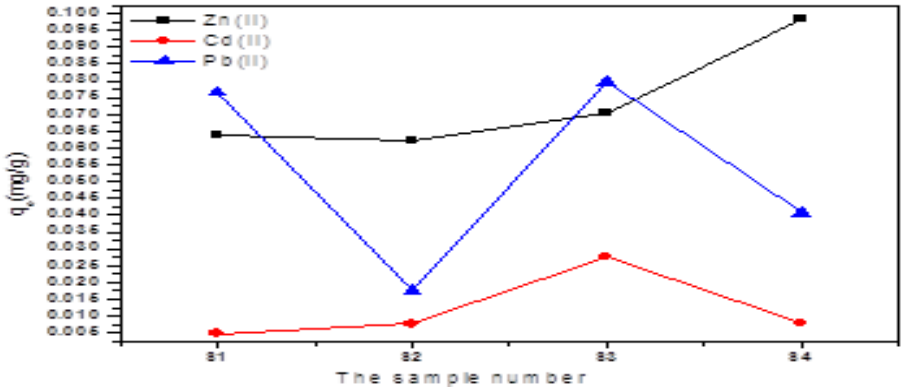

Fig. 8: The metal ion uptake from different source using amberjet 1500H

Table 10 shows the metal ion concentration of the untreated and the maximum removal percentage (%) of eleven metal ion. As can be seen, more than 99.84, 98.41, 97.78 and 99.60 % of Zn (II) was removed from samples S1, S2, S3 and S4, respectively, 98.00, 96.25, 95.97 and 98.75 % of Cd (II) was removed from samples S1, S2, S3 and S4, respectively, and 95.88, 98.33, 99.50 and 99.27 % of Pb (II) was removed from samples S1, S2, S3 and S4, respectively and other metal ions was significantly treated. Thus, the Amberjet 1500H is an efficient and cost-effective adsorbent for eliminating Zn(II), Cd(II), Pb(II) and other contaminants from industrial wastewaters, in addition to surface and groundwaters.

Table 10: The initial metal ion concentration and the maximum removal percentage

The Metal Ion	The Sample Number							
	S1		S2		3		S4	
	ppm	%	ppm	%	ppm	%	Ppm	%
Al(III)	1.7	94.53	0.39	98.46	0.45	98.44	0.09	93.33
Ba(II)	0.31	97.10	0.041	97.56	0.088	97.73	0.053	98.11
Cd(II)	0.05	98.00	0.08	96.25	0.29	95.97	0.08	98.75
Cr(III)	0.3	99.67	0.02	95.00	0.05	94.00	0.02	95.00
Co(II)	0.08	96.25	0.004	25.00	0.17	97.06	0.09	95.56
Cu(II)	0.97	96.91	0.85	98.00	0.67	98.66	0.50	98.40
Fe(III)	1.6	99.50	0.5	96.00	0.94	98.94	1.24	99.27
Pb(II)	0.8	95.88	0.18	98.33	0.8	99.50	0.41	99.27
Mn(II)	0.26	98.08	0.21	97.14	0.19	86.84	0.19	97.37
Ni(II)	0.98	99.90	0.14	98.57	0.04	92.50	0.06	96.67
Zn(II)	0.64	99.84	0.63	98.41	0.72	97.78	0.99	99.60

Conclusion

The adsorption of cadmium onto Amberjet 1500H strong-acid cation exchange resin has been investigated on the basis of the feed batch cadmium concentration and contact time effects. The aim of the studies was to examine the potential of this ion exchange resin towards the removal of Cd (II) from synthetic wastewater.

The achieved results reveal that the removal efficiency of Cd (II) increases as the concentration of cadmium in the feed increases. The equilibrium was reached after 240 min and from this point forward the removal efficiency was about 94.03 %. Thereby, the concentration of this compound in the eluted solution after ion exchange was agree with the legislated limits for reuse of the purified effluent. This means that Amberjet 1500H strong-acid cation exchange resins exhibits very significant

potential for the removal of metal ions and also from other contaminated wastewaters over a wide range of concentrations.

On the other hand, a thorough thermodynamic study of the ion exchange process has been performed. The equilibrium behavior of this pollutant has been accurately predicted by Langmuir isotherm ($R^2 > 0.999$). Furthermore, pseudo-first order, pseudo-second order and intraparticle and film diffusion models have been employed to predict the kinetics of cadmium adsorption on the resin. The results show that the correlation coefficients of the second-order model were the highest, indicating that this model describes with utmost accuracy the adsorption of cadmium onto this resin.

References

Alzaydien, A.S., 2009. J. Am, Appl. Sci., 5: 197-208.
Anirudhan, T.S., P.G. Radhakrishnan, 2008. J. Chem, Thermody., 40: 702-709.
Apak, R., E. Tutem, M. Hugul, J. Hizal, 1998. Water Res., 32: 430-440.
Arup Roy, Jayanta Bhattacharya; 2013. Sep. Pur. Technol., 115: 172-179.
Barbier, O., G. Jacquillet, M. Tauc, M. Cougnon, P. Poujeol, 2005. Nephron Physiol., 99: 105-110.
Boyd, E.G., A.W. Adamson, L.S. Meyers, 1947. J. Am. Chem. Soc., 69: 2836-2848.
Bruno, H., S. Luciana Rocha, B. Cláudia Lopes, A.C. Paula Figueira, Duarte, M.A. Carlos Vale, E. Pardal, Pereira; 2017. J. Environm. Managem., 191: 275-289.
Cheng, Z., W. Ma, L. Gao, Z. Gao, R. Wang, J. Xu, 2014. Desalination Water Treat, 52: 5663-5672.
Dinesh, M., K. Sandeep, S. Anju, 2014. Ecological Eng., 73: 798-808.
Dubinin, M.M., L.V. Radushkevich, 1947. Chemisches Zentralblatt, 1: 875-890.
Edidiong, A., Alastair Martin, Petrus Nzerem, Flor Siperstein, Xiaolei Fan; 2017. J. Environm. Chem. Eng., 5: 679-698.
Elkady, M.F., M.M. Mahmoud, H.M. Abd-EI-Rahman, 2011. J Non-Cryst Solids, 357: 1118-1129.
Elmorsi, T.M., 2011. J. Environ, Protect., 2: 817-827.
Ensieh, G., Akbar Heydari, Mika Sillanpää; 2017.Microchemical J., 13: 51-56.
Fang, Z., Luwei Li, Junde Xing; 2017 .J.Hazard. Mater., 321(5): 103-110.
Freundlich, H., 1906. Zeitschrift für Physikalische Chemie, 57: 384-470.
Hamid H., G.G. Hossein, T.M. Meisam, H. Amir, 2014. J. Dispers. Sci. Technol., 35(4): 501-509.
Helfferich, F.G., 1962. Ion Exchange McGraw Hill Book Company, New York.
Hemmati, 2015. Desalination Water Treat, 53: 149-157.
Ho, Y.S., G. Mckay, 1998. Trans. I Chem. E, 76B: 332-340.
Ho, Y.S., 2006. Water Res., 40: 119-125.
Ho, Y.S., G. McKay, 2000. Water Research, 34: 735-742.
Ho, Y.S., G. McKay, 1999. Process Biochem., 34: 735-742.
Huacai, G., W. Jincui, 2017. Chemosphere, 169: 443-449.
Järup, L., 2003. Br. Med. Bull., 68: 167-182.
Joyce, S. Clemente, Suzanne Beauchemin, Ted MacKinnon, Joseph Martin, Cliff T. Johnston, Brad Joern; 2017.Chemosphere, 170: 216-224.
Kazutoshi, S., K. Takashi, 2012. Appl. Clay Sci., 62-63: 58-62.
Kosa, S.A., G. Al-Zhrania, M.A. Salam, 2012. Chem Eng J, 181-182: 159-168.
Lagergren, S., 1898. Kungliga Svenska Vetenskapsakademiens, Handlingar, 24: 1-39.
Langmuir, I., 1918. J.Am. Chem. Soc., 57: 1361-1403.
Lu, L., Xuesong Xu, Charalambos Papelis, Pei Xu, 2017.Chemical Engineering Research and Design, 120: 231-239.
Mayesa, W.M., H.A.B. Potterb, A.P. Jarvis, 2009. J. Hazard. Mater., 162: 512-520.
McManamon, C., A.M. Burke, J.D. Holmes, M.A. Morris, 2012. J Colloid Interf Sci., 369: 330-337.
Mohamad, A., Fulazzaky, Zohreh Majidnia, Ani Idris; 2017.Chem.Eng.J. 308(15): 700-709
Mohammad, Y., Masoomi, Minoo Bagheri, Ali Morsali; 2017.Ultrasonics Sonochemistry, 37: 244-250.
Mohammadi, M., A. Ghaemi, M. Torab-Mostaedi, M. Asadollahzadeh, A. Kulkarni R.M., K.V. Shetty, G. Srinikethan, 2014. J Taiwan Inst Chem Eng, 45: 1628-1635.
Nguyen, V.C., Q.H. Phop, 2014. Sci. World J., pp: 273082-273091.

Ould, B.I., I.M. Belmedani, A. Belgacem, H.Z. Hadoun, Z. Sadaoui, 2014. Chem. Eng. Trans., 38: 121-126.
Prasad, M., S. Saxena, 2004. Ind. Eng. Chem. Res., 43: 1512-1522.
Rajab, A., Sami A. Zabin, 2017. J.Taibah University for Sci., 11: 57-65.
Rangel-Mendez, J.R., R. Monroy-Zepeda, E. Leyva-Ramos, P.E. Diaz-Flores, K. Shirai, 2009. J Hazard. Mater., 162: 503-511.
Reichenberg, D., 1953. J. Am. Chem. Soc., 75: 589-597.
Sagnik, C., Shamik Chowdhury, Papita Das Saha; 2011.Carbohyd. Polym., 86: 1533-1541.
Shek, T.-H., A. Ma, V.K.C. Lee, G. McKay, 2009. Chem. Eng. J., 146: 63-70.
Singh, B., S.K.D as, Colloids and Surf. B: 2013. Biointer., 107: 97-106.
Temkin, I.M., V. Pyzhev, 1940. Acta Physiochem. SSR 12: 217-222.
The World Health Organization (WHO), 2008. Guidelines for drinking-water quality: recommendations-addendum (3rd end), 1.
Ting, W., Wen Liu, Lin Xiong, Nan Xu, Jinren Ni; 2013.Chem. Eng. J. 215-216: 366-374.
World Health Organization, Copenhagen, 2007.
Yavari, R., S.J. Ahmadi, Y.D. Huang, A.R. Khanchi, G. Bagheri, J.M. He, 2009. Talanta, 77: 1179-1184.
Weber, W.J., J.C. Morris, 1963. Journal of the Sanitary Engineering Division - American Society of Civil Engineers, 89: 31-60.
Zahra, M.,. Sun Shangbin, Cory Berkland, Jenn-tai Liang, 2017.Chem.Eng. J., 307: 496-502.
Zeldowitsch, J., 1934. Acta Physicochim. URSS, 1: 364-449.
Zhang, H., Wang Xiaoyun, Liang Honghong, Tan Tianshe, Wu Wangsuo; 2016. Appl. Clay Sci., 127-128.